


RESEARCH

Open Access



Accelerated directed evolution of dye-decolorizing peroxidase using a bacterial extracellular protein secretion system (BENNY)

Abdulrahman H. A. Alessa^{1†}, Kang Lan Tee^{1*†}, David Gonzalez-Perez¹, Hossam E. M. Omar Ali¹, Caroline A. Evans¹, Alex Trevaskis¹, Jian-He Xu² and Tuck Seng Wong^{1*} 

Abstract

Background: Dye-decolorizing peroxidases (DyPs) are haem-containing peroxidases that show great promises in industrial biocatalysis and lignocellulosic degradation. Through the use of *Escherichia coli* osmotically-inducible protein Y (OsmY) as a bacterial extracellular protein secretion system (BENNY), we successfully developed a streamlined directed evolution workflow to accelerate the protein engineering of DyP4 from *Pleurotus ostreatus* strain PC15.

Result: After 3 rounds of random mutagenesis with error-prone polymerase chain reaction (epPCR) and 1 round of saturation mutagenesis, we obtained 4D4 variant (I56V, K109R, N227S and N312S) that displays multiple desirable phenotypes, including higher protein yield and secretion, higher specific activity (2.7-fold improvement in k_{cat}/K_m) and higher H₂O₂ tolerance (sevenfold improvement based on IC₅₀).

Conclusion: To our best knowledge, this is the first report of applying OsmY to simplify the directed evolution workflow and to direct the extracellular secretion of a haem protein such as DyP4.

Keywords: Directed evolution, Extracellular protein secretion, Dye-decolorizing peroxidase, Osmotically-inducible protein Y, Hydrogen peroxide tolerance

Introduction

Dye-decolorizing peroxidases (DyPs; PF04261; EC 1.11.1.19) comprise a recently described family of haem peroxidase enzymes, which is unrelated to the super-families of plant and animal peroxidases (Martinez et al. 2017). According to the RedoxiBase [<http://peroxibase.toulouse.inra.fr/>; accessed on 07/04/19, (Fawal et al. 2013)] a total of 237 DyPs have been identified in the genomes of fungi, bacteria and archaea. Although their physiological functions are yet to be fully elucidated, DyPs have several characteristics that distinguish them from all other peroxidases. They exhibit low sequence

similarity to the classical fungal peroxidases, such as lignin peroxidase (LiP; EC 1.11.1.14) and manganese peroxidase (MnP; EC 1.11.1.13). Structural characterization of DyPs revealed the presence of a two-domain, $\alpha + \beta$ ferredoxin-like fold that is distinct from the all α -helical fold of the other peroxidase superfamilies (Singh and Eltis 2015). Initial structure- and sequence-based alignments identified four phylogenetically distinct classes of DyPs (A to D). Classes A to C predominantly contain bacterial sequences while class D is mostly represented by fungal DyPs. DyPs are bifunctional enzymes displaying not only oxidative activity but also hydrolytic activity (Hofrichter et al. 2010). They show a particularly wide substrate range and function well under much lower pH conditions compared to other plant peroxidases. They are also able to oxidize a variety of organic compounds of which some are poorly converted by established peroxidases, including dyes (e.g. anthraquinone-based industrial dyes), β -carotene and aromatic sulphides.

*Correspondence: k.tee@sheffield.ac.uk; t.wong@sheffield.ac.uk

[†]Abdulrahman H. A. Alessa and Kang Lan Tee contributed equally to this work

¹Department of Chemical & Biological Engineering and Advanced Biomanufacturing Centre, University of Sheffield, Sir Robert Hadfield Building, Mappin Street, Sheffield S1 3JD, UK

Full list of author information is available at the end of the article

Accumulating evidence shows that DyPs play a key role in lignin degradation. Owing to these unique properties, DyPs are potential candidates for a variety of biotechnological applications.

In this article, we enhanced the hydrogen peroxide (H₂O₂) tolerance of dye-decolorizing peroxidase 4 (DyP4) from *Pleurotus ostreatus* strain PC15 (oyster mushroom) using directed evolution. DyP4 was the first reported fungal DyP capable of oxidizing manganese (II) (Fernandez-Fueyo et al. 2015). Additionally, it oxidizes both low and high redox-potential dyes. It also displays high thermal and pH stability. DyP4 was detected in the secretome of *P. ostreatus* grown on different lignocellulosic substrates, suggesting that the generation of Mn³⁺ oxidizers plays a role in the *P. ostreatus* white-rot lifestyle.

To accelerate DyP4 evolution, we used a bacterial extracellular protein secretion system (BENNY) based on the *Escherichia coli* osmotically-inducible protein Y (OsmY). OsmY was originally identified as a naturally excreted protein in a systematic proteomic analysis of the extracellular proteome of *E. coli* BL21 (DE3) (Qian et al. 2008). It was subsequently used as a fusion partner to direct the extracellular secretion of various recombinant proteins expressed in *E. coli*, including endoglucanase (Gupta et al. 2013), β -glucosidase (Gupta et al. 2013), xylanase (Zheng et al. 2012; Le and Wang 2014), xylosidase (Zheng et al. 2012), single-chain antibody (Cheng et al. 2014) and various human proteins (Kotzsch et al. 2011). To our best knowledge, this is the first report of applying OsmY to streamline directed evolution workflow and to direct extracellular secretion of a haem protein such as DyP4.

Materials and methods

Materials

Chemicals were purchased from Sigma-Aldrich (Dorset, UK) and ForMedium (Norfolk, UK). DNA modifying enzymes, deoxyribonucleotides and DNA ladders were purchased from New England Biolabs (Hitchin, UK), Thermo Fisher Scientific (Loughborough, UK) and Agilent Technologies (Cheadle, UK). Nucleic acid purification kits were purchased from Qiagen (Manchester, UK), Machery-Nagel (Düren, Germany) and Omega Bio-tek (Norcross, USA). All oligonucleotides were synthesized by Eurofins Genomics (Ebersberg, Germany) and summarized in Table 1.

Strains

Escherichia coli DH5 α was used for all molecular cloning, plasmid propagation and maintenance. *E. coli* BL21 (DE3) (Merck; Darmstadt, Germany) was used for DyP4 and OsmY-DyP4 protein expression.

Molecular cloning of DyP4 and OsmY-DyP4

The DNA sequence encoding both the *E. coli* osmotically-inducible protein Y (OsmY; GenBank: AU30809.1) and the *Pleurotus ostreatus* strain PC15 dye-decolorizing peroxidase 4 (DyP4; GenBank: KP973936.1) was codon-optimized for protein expression in *E. coli* and synthesized by GenScript (Piscataway, USA). The gene (Additional file 1: Figure S1) was cloned into pET-24a(+) vector (Merck; Darmstadt, Germany) using *NdeI* and *EcoRI* sites, and the resulting plasmid [pET-24a(+)-OsmY-DyP4; Additional file 1: Figure S2] was used for protein engineering in this study. To create pET-24a(+)-DyP4 plasmid, DyP4 gene was amplified with *NdeI*-DyP4-Fwd and DyP4-Rev primers, digested with *NdeI* and *EcoRI* and cloned into pET-24a(+) vector.

Random mutagenesis by epPCR

Three error-prone polymerase chain reaction (epPCR) conditions were used in this study: high (H), medium (M) and low (L) error rates. For epPCR of high error rate, the 50- μ L PCR mixture contained 1 \times standard Taq reaction buffer (Mg-free), 7 mM MgCl₂, 0.05 mM MnCl₂, 0.2 mM of each dNTP, 20 pmol BamHI-DyP4-Fwd primer, 20 pmol DyP4-Rev primer, 50 ng pET-24a(+)-OsmY-DyP4 and 1.25 U Taq DNA polymerase (New England Biolabs). For epPCR of medium error rate, the 50- μ L PCR mixture contained 1 \times standard Taq reaction buffer (Mg-free), 7 mM MgCl₂, 0.2 mM dATP, 0.2 mM dGTP, 1 mM dTTP, 1 mM dCTP, 20 pmol BamHI-DyP4-Fwd primer, 20 pmol DyP4-Rev primer, 50 ng pET-24a(+)-OsmY-DyP4 and 1.25 U Taq DNA polymerase (New England Biolabs). For epPCR of low error rate, the 50- μ L PCR mixture contained 1 \times standard Taq reaction buffer (Mg-free), 1.5 mM MgCl₂, 0.01 mM MnCl₂, 0.3 mM of each dNTP, 4.5 pmol BamHI-DyP4-Fwd primer, 4.5 pmol DyP4-Rev primer, 3.5 ng pET-24a(+)-OsmY-DyP4 and 1.25 U Taq DNA polymerase (New England Biolabs). The PCR mixtures were thermocycled using the following conditions: (i) 30 s initial denaturation at 95 °C, (ii) 30 cycles of 20 s denaturation at 95 °C, 30 s annealing at 68 °C and 1 min 30 s extension at 68 °C and (iii) 5 min final extension at 68 °C. PCR products were either purified by gel extraction (high and medium error rate) or PCR purification following *DpnI* digestion (low error rate). After restrictive digestion with *BamHI* and *EcoRI*, the PCR products were cloned into pET-24a(+)-OsmY vector. The recombinant plasmids were subsequently electroporated into *E. coli* BL21 (DE3) to create OsmY-DyP4 mutant libraries.

Cultivation and protein expression in 96-well microtitre plates

Individual colonies were picked manually using sterile toothpicks into 96-well microtitre plates, with each well

Table 1 Oligonucleotides used in this study

Oligonucleotide	Applications	DNA sequence (5'–3')
Ndel-DyP4-Fwd	Cloning	TATACATATGATGACCACCCCGGCCGCCGCTG
DyP4-Rev	Cloning, epPCR, SM	ATGCGAATTCTTACGCGCTGATCGGCGCTTGGCTGTGC
BamHI-DyP4-Fwd	epPCR, SM	GATCGGATCCATGACCACCCCGGCCGCCGCTGG
M43L-F	SDM	AAAGCGAACCTGGCGCACTTCATCCCGCACATTAAGACCAGCGCGG
M43L-R	SDM	GAAGTGCGCCAGGTTTCGCTTTAAATTGATCAACGTTGGTCACGTGC
M77L-F	SDM	CTGGTCCGCTGGCGCGGTGAACGTTAGCTTTAGCCACCTGGGCC
M77L-R	SDM	CACCGCCGCCAGCGGCACCAGACCCGGTTTCTTCTGACGTTTGTGT
M253L-F	SDM	CTGTTCCAACCTGGTGCCGAGTTTGACGATTTCTGGAAAGCAACC
M253L-R	SDM	CTCCGGCACCAGTTGGAACAGGTAACGGAAGGTCAGAAAGCTACCA
M253F-F	SDM	CTGTTCCAATTTGTGCCGAGTTTGACGATTTCTGGAAAGCAACC
M253F-R	SDM	CTCCGGCACAAATTGGAACAGGTAACGGAAGGTCAGAAAGCTACCA
NOP-312N-F	SM	TGCGCAGCGTNNKAACAAGTTTGACTTC
NOP-312N-R	SM	TCCGCCGCCAGTTTCGGATCGTCCT
4P-56N-F	SM	ACCAGCGCGGCCNNKATTAAGACCGTGAG
4P-56N-R	SM	TTAATMNNGCCCGCTGGTCTTAATGTG
4P-109N-F	SM	ACCGGCCAGCGTNNKGACGCGGAGATTCTG
4P-109N-R	SM	CGCGTCMNNACGCTGGCCGGTGGTGAACGC
4P-227N-F	SM	CTGGCGAAGGAGNNKGGTGACAGCCGTGCG
4P-227N-R	SM	GTCACCMNNCTCCTTCGCCAGAATGAAACC
4P-306N-F	SM	GATCCGAAACTGNNKCGGATGCGCAGCGT
4P-306N-R	SM	ATCCGCMNNCAGTTTCGGATCGTCCTTCAG
4P-374N-F	SM	ACCAGCCAAGAANNKACGACAAGAAACC
4P-374N-R	SM	GTCGTGMNNTTCTTGCTGGTCACTCCGG

epPCR error-prone polymerase chain reaction, SDM site-directed mutagenesis, SM saturation mutagenesis

containing 150 μ L 2 \times TY medium (16 g/L tryptone, 10 g/L yeast extract and 5 g/L NaCl) supplemented with 50 μ g/mL kanamycin. Wells B2, E6 and G11 were inoculated with either wildtype (WT) or parental strain as internal control. Plates were covered with lids, sealed and cultivated at 30 $^{\circ}$ C for 24 h. Following cultivation, 100 μ L of 50% (v/v) glycerol solution was added to each well, and these master plates were stored at -80° C.

To prepare pre-culture for protein expression, master plates were replicated using a pin replicator into fresh 96-well microtitre plates, with each well containing 150 μ L 2 \times TY medium supplemented with 50 μ g/mL kanamycin. These pre-culture plates were grown at 30 $^{\circ}$ C for 18 h, before being used to inoculate fresh 96-well microtitre plates, with each well containing 150 μ L 2 \times TY-based auto induction medium [AIM; 16 g/L tryptone, 10 g/L yeast extract, 3.3 g/L (NH₄)₂SO₄, 6.8 g/L KH₂PO₄, 7.1 g/L Na₂HPO₄, 0.5 g/L glucose, 2.0 g/L α -lactose and 0.15 g/L MgSO₄] supplemented with 50 μ g/mL kanamycin. After cultivation at 30 $^{\circ}$ C for 24 h, the plates were centrifuged at 4000 rpm (eq. 2342 g) for 10 min. The spent medium containing secreted OsmY-DyP4 was used for high-throughput screening (HTS).

Abgene 96-well polypropylene storage microplates (Thermo Fisher Scientific; AB0796) and Abgene polypropylene plate covers (Thermo Fisher Scientific; AB0755) were used in preparing master plates, pre-culture plates and protein expression plates. All plate cultivations were conducted in Titramax1000 plate shaker coupled to an Incubator 1000 heating module (Heidolph Instruments; Essex, UK) using a shaking speed of 1050 rpm.

Screening for higher H₂O₂ tolerance

Flat-bottom clear 96-well polystyrene microplates (Greiner Bio-One; 655161) were used for screening. Twenty microlitre of spent medium was transferred to 96-well microtitre plate, with each well containing 150 μ L of 10 mM 2,2'-azino-bis(3-ethylbenzothiazoline-6-sulphonic acid) (ABTS) prepared in 0.1 M citrate–0.2 M Na₂HPO₄ pH 3.4 buffer solution. The mixture was shaken for 2 min before reaction was initiated by adding 50 μ L of 17.5 mM H₂O₂ solution. Absorbance at 405 nm was recorded with Multiskan FC microplate photometer (Thermo Fisher Scientific), after a 2-min reaction with shaking. All solutions were freshly prepared prior to screening. All shaking steps were conducted in Titramax

1000 (Heidolph Instruments) using a shaking speed of 1050 rpm.

Site-directed mutagenesis and saturation mutagenesis

Mutagenic primers (Table 1), PCR mixtures and PCR conditions for all site-directed mutagenesis and saturation mutagenesis studies were designed using OneClick programme, which is publicly accessible via the web-link: <http://tucksengwong.staff.shef.ac.uk/OneClick/> (Warburton et al. 2015).

All methionine-substituted variants were created using pET-24a(+)-DyP4 as template. To construct M43L (primers M43L-F and M43L-R), M253L (primers M253L-F and M253L-R) and M253F (primers M253F-F and M253F-R) variants, partially overlapping primers and Q5 high-fidelity DNA polymerase (New England Biolabs) were used in a 2-stage PCR. To construct M77L variant (primers M77L-F and M77L-R), DNA polymerase used was substituted with PfuUltra high-fidelity DNA polymerase AD (Agilent Technologies).

Saturation mutagenesis was performed on positions 56, 109, 227, 306, 312 and 374 of DyP4 using pET-24a(+)-OsmY-DyP4 variant 3F6 as template. For position 312, non-overlapping primers were used (Table 1). For positions 56, 109, 227, 306 and 374, a 4-primer method was applied using 2 flanking primers (BamHI-DyP4-Fwd and DyP4-Rev) and 2 internal primers (Table 1). Q5 high-fidelity DNA polymerase (New England Biolabs) was used in all PCRs.

Protein expression and purification

For protein expression, plasmid was freshly transformed into *E. coli* BL21 (DE3). Cells were grown in 2× TY media supplemented with 50 µg/mL kanamycin at 37 °C. When OD₆₀₀ reached 0.5–0.6, 1 mM isopropyl β-D-1-thiogalactopyranoside (IPTG) was added to induce protein expression and temperature was lowered to 25 °C. After 24 h, cells were harvested and pellets were stored at – 20 °C.

For protein purification, cells were resuspended in pre-chilled buffer A (50 mM Tris–HCl pH 8.5, 1 mM EDTA) supplemented with DNase, RNase, protease inhibitor and lysozyme, and were lysed by sonication (Vibra-Cell ultrasonic liquid processors; Sonics & Materials; Newtown, USA). Lysed cells were centrifuged and supernatant was loaded onto a 5-mL HiTrap Q HP anion exchange chromatography column (GE Healthcare Life Sciences; Pittsburgh, USA) pre-equilibrated with buffer A. After washing with 5 column volumes (CVs) of buffer A, protein was eluted with a linear gradient of NaCl (0–1 M) in buffer A. Protein was subsequently diluted 10× with buffer B (25 mM acetate pH 4.0) to adjust the NaCl concentration, before loading onto a 5-mL HiTrap SP HP cation exchange chromatography column (GE Healthcare

Life Sciences) pre-equilibrated with buffer B. After washing with 5 CVs of buffer B, protein was eluted with a linear gradient of NaCl (0–1 M) in buffer B. Fractions containing target protein were pooled and loaded onto HiLoad 26/600 Superdex 75 pg column (GE Healthcare Life Sciences) pre-equilibrated with buffer C [0.1 M citrate–0.2 M Na₂HPO₄ pH 4.0, 100 mM NaCl, 10% (v/v) glycerol]. Purified DyP4 protein was immediately flash cooled in liquid nitrogen and stored in – 80 °C.

UV-visible spectroscopy and concentration measurement of purified DyP4 WT and variants

Purified DyP4 stored at – 80 °C was thawed and transferred to a quartz cuvette. UV-visible spectra were collected using a UV-3100PC spectrophotometer (VWR; Lutterworth, UK). Spectra between 250–800 nm were recorded at ambient temperature for all proteins in buffer C, typically at concentrations of 3–6 µM. DyP4 protein concentration was calculated based on absorbance at 280 nm, measured using the BioPhotometer Plus (Eppendorf; Stevenage, UK), and an extinction coefficient of 29,575 M⁻¹ cm⁻¹ (calculated using ProtParam).

Kinetic constants of DyP4 WT and variants

The kinetic constants of DyP4 were determined for ABTS oxidation. All ABTS stock solutions were prepared in 0.1 M citric acid–0.2 M Na₂HPO₄ buffer pH 3.4 and 1 mM hydrogen peroxide was prepared in deionised water. The assay was performed at ambient temperature in flat-bottom clear 96-well polystyrene microplates (Greiner Bio-One; 655161). 140 µL of ABTS stock solution (final concentrations of 0.1–7.0 mM) was transferred to the microtitre plate before 10 µL of purified DyP4 (final concentrations of 0.1–0.2 µM) was added. The reaction was initiated by 50 µL of 1 mM H₂O₂ and formation of ABTS cation radical was recorded at 405 nm [$\epsilon_{405} = 36.8 \text{ mM}^{-1} \text{ cm}^{-1}$, (Otieno et al. 2016)] with Multiskan FC microplate photometer (Thermo Fisher Scientific). All experiments were performed in triplicates. The Michaelis constants (K_m and V_{max}) were obtained by non-linear regression analysis to the Michaelis–Menten model using GraphPad Prism (GraphPad Software; San Diego, USA). The catalytic rate (k_{cat}) was calculated using $k_{cat} = V_{max} / (\text{DyP4 concentration})$.

Hydrogen peroxide tolerance of DyP4 and variants

The hydrogen peroxide tolerance for DyP4 was determined using ABTS oxidation. Assay procedure is similar to the determination of DyP4 kinetic constants, except 7 mM ABTS in 0.1 M citric acid–0.2 M Na₂HPO₄ buffer pH 3.4 and 0.15–50.00 mM H₂O₂ were used. All reaction rates were normalized against the reaction rate at 0.25 mM H₂O₂ for the respective DyP4 wildtype or

variants. All experiments were performed in triplicates. The residual activity was plotted against H_2O_2 concentration and non-linear regression analysis to the “[inhibitor] vs. response—variable slope (four parameter)” model was performed using GraphPad Prism (GraphPad Software) to obtain IC_{50} values of H_2O_2 .

Acetone precipitation of protein

One volume of spent medium (350 μ L) was mixed with 4 volumes of acetone (1400 μ L) that was pre-chilled at -20 °C. The mixture was vortexed thoroughly and incubated at -80 °C for 15 min, before overnight incubation at -20 °C. Subsequently, the mixture was centrifuged at 21,000 g and 4 °C for 15 min. After decanting the supernatant, residual acetone was allowed to evaporate at room temperature for 30 min. Protein pellet was dissolved in 35 μ L of $1\times$ SDS sample loading buffer and 20 μ L of protein sample was analysed by SDS-PAGE.

Proteomic analysis

Proteins present in SEC fractions 2 and 7 were first resolved by SDS-PAGE. Gel bands were excised from the SDS-PAGE gel manually, post visualization by Coomassie blue stain. The gel bands were then de-stained and proteolytically digested with trypsin to generate peptides for mass spectrometry analysis (Shevchenko et al. 2006) using liquid chromatography LC-MS/MS. Mascot software search engine was employed to process the mass spectrometry data to identify proteins from the peptide sequence reference database for *Escherichia coli* (strain B/BL21-DE3) (UniProt Proteome ID: UP000002032; 4156 entries; downloaded on 07/04/2019). The sequence of the recombinant OsmY-DyP4 protein was included as an additional entry to this reference proteome.

Results and discussion

Methionine substitution did not improve H_2O_2 tolerance of DyP4

Peroxidases use H_2O_2 as the electron acceptor to catalyse numerous oxidative reactions. For DyP4, the optimum H_2O_2 concentration for ABTS oxidation was determined to be 0.25 mM. This was consistent with a previous study that used exactly the same H_2O_2 concentration for the oxidation of ABTS, Mn^{2+} , Reactive Blue 19 (RB19), Reactive Black 5 (RB5) and 2,6-dimethoxyphenol (DMP) (Fernandez-Fueyo et al. 2015). Other DyPs operate optimally in similar H_2O_2 concentration range. For example, 0.2 mM H_2O_2 was used for ABTS, guaiacol and DMP oxidation by bacterial DyP from *Pseudomonas putida* MET94 (PpDyP) (Brissos et al. 2017). DyP from cyanobacterium *Anabaena* sp. strain PCC 7120 (AnaPX) functioned optimally at 0.4 mM H_2O_2 for RB5 oxidation (Ogola et al. 2009). For DyP from *Irpex lacteus*, the

optimum H_2O_2 concentration for ABTS oxidation was between 0.4 and 0.8 mM (Salvachua et al. 2013).

As with other DyPs, DyP4 is inhibited by H_2O_2 . In an attempt to enhance the H_2O_2 tolerance of DyP4, we created 4 methionine-substituted variants (M43L M77L M253L and M253F). Our decision was guided by two reasons: (1) The amino acids methionine, cysteine, histidine, tryptophan and tyrosine are typical targets for oxidation within proteins due to the high reactivity of sulphur atoms and aromatic rings towards various reactive oxygen species (Li et al. 1995), and (2) Ogola et al. successfully enhanced the H_2O_2 stability of AnaPX by 2.4- to 8.2-folds through substituting methionine residues with high redox residues such as isoleucine, leucine and phenylalanine (Ogola et al. 2010).

Although all 4 methionine-substituted variants were properly folded judging by the absorption spectra of the purified proteins and were catalytically active, there was no improvement in their H_2O_2 tolerance (data not shown). This result prompted us to apply directed evolution to enhance H_2O_2 tolerance.

N-terminal OsmY fusion resulted in extracellular DyP4 secretion

In directed evolution using *E. coli* as protein expression host, protein variants are often expressed in 96-well format. Prior to enzymatic assays, cells are lysed to release recombinant proteins using physical (e.g. freeze-thaw cycle), chemical (e.g. polymyxin B, Triton X-100, Tween 20, NP40, CHAPS and cholate etc.), enzymatic (e.g. lysozyme) or combinations of these approaches. In engineering PpDyP using directed evolution, for instance, *E. coli* cells were disrupted through multiple steps to release DyP enzymes: (i) cell harvest by centrifugation, (ii) physical-enzymatic treatment (freeze at -80 °C for 15 min, thaw at 30 °C for 5 min, re-suspension in buffer containing lysozyme) and (iii) cell debris removal by centrifugation (Brissos et al. 2017).

To streamline the DyP4 directed evolution workflow, we fused *E. coli* OsmY to the N-terminus of DyP4 and investigated protein secretion using 2 expression hosts [*E. coli* BL21 (DE3) and *E. coli* C41 (DE3)] and 2 protein expression temperatures (30 °C and 37 °C) in $2\times$ TY-based AIM. Using ABTS assay, we confirmed extracellular OsmY-DyP4 secretion and *E. coli* BL21 (DE3) was superior to *E. coli* C41 (DE3) based on the activity of secreted protein. In addition, an expression temperature of 30 °C resulted in higher protein secretion. By using OsmY as secretory carrier and fusion protein expression in AIM, we bypassed both (i) protein induction (i.e. addition of IPTG inducer) and (ii) cell disruption, which allows us to develop a far more elegant HTS as depicted in Additional file 1: Figure S3. Worthy of a mention, in

addition to DyP4, OsmY was also a good carrier protein for β -glucosidase (53 kDa) and lipase (20 kDa) (unpublished data).

Accelerated HTS with BENNY

After confirming the extracellular secretion of OsmY-DyP4 using BENNY, we adapted this to 96-well format (Additional file 1: Figure S3). Based on ABTS assay, we obtained an apparent coefficient of variance (CV) of 8% for OsmY-DyP4 (Fig. 1 and Additional file 1: Figure S4). Concurrently, we cultivated *E. coli* BL21 (DE3) carrying no plasmid in a 96-well plate (denoted as background plate) to calculate the background absorbance. After subtracting the background absorbance ($Abs_{405} = 0.2427$), we obtained a true CV of 22%. The increase in Abs_{405} of 0.1425, on average, was therefore due solely to the enzymatic oxidation of ABTS by the secreted OsmY-DyP4.

A closer look at both the assay plate and the background plate revealed that the deviation was mainly caused by liquid evaporation from bordering wells, which resulted in higher secreted protein concentration in these wells (Additional file 1: Figure S4). If all bordering wells were excluded, the apparent and true CVs were reduced to 4% and 11%, respectively.

Therefore, BENNY-assisted ABTS assay was well suited for directed evolution to differentiate and identify improved protein variants. Worthy of note, in order to isolate OsmY-DyP4 variants of enhanced H_2O_2 tolerance, we intentionally increased the H_2O_2 concentration in our assay from 0.25 to 4 mM, representing a 16 \times increase. At 4 mM H_2O_2 , DyP4 WT showed a relative activity of $\sim 30\%$, compared to that at 0.25 mM H_2O_2 .

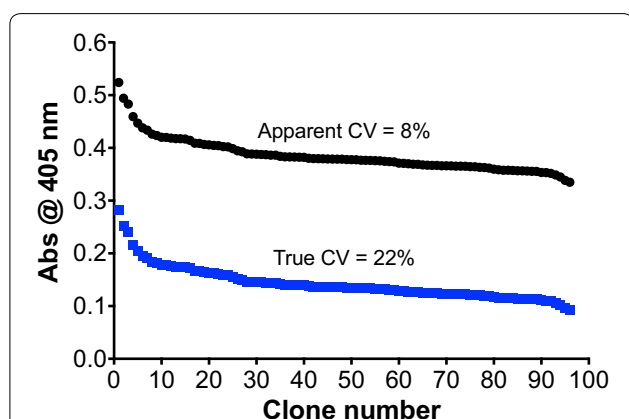


Fig. 1 Activity values (Abs_{405}) of OsmY-DyP4-catalysed ABTS oxidation in a 96-well plate, reported in a descending order (black—before background subtraction, blue—after background subtraction). The assay was conducted using a protocol streamlined with OsmY-based BENNY. The apparent coefficient of variance (CV) was calculated without subtracting the assay background, while the true CV was obtained after background subtraction

Random mutagenesis by epPCR

As this was our first directed evolution attempt on DyP4, we created random mutagenesis libraries of OsmY-DyP4 using 3 epPCR conditions (H, M and L). Important to note, mutations were only targeted to the sequence encoding for DyP4, leaving the OsmY sequence unaltered. The error rate of Taq DNA polymerase was manipulated by increasing Mg^{2+} concentration, adding Mn^{2+} , applying imbalanced nucleotide concentration or utilizing combinations of these factors (Wong et al. 2006). As evidenced in Fig. 2a, at high and medium error rates, we observed a reduction in the PCR product yield and appearance of multiple side products. Therefore, combining increased Mg^{2+} concentration and Mn^{2+} addition (condition H) gave the highest error rate. A combination of increased Mg^{2+} concentration and imbalanced nucleotide concentration (condition M) gave the medium error rate. Finally, adding 0.01 mM Mn^{2+} alone (condition L) gave the lowest error rate.

This was further confirmed by screening these epPCR libraries using BENNY-assisted ABTS assay (Fig. 2b). Most of the clones (77.42%; Additional file 1: Figure S5) in the library prepared with condition H were either inactive or not as active as the parental strains (wells B2, E6 and G11). These percentages were much lower in the libraries prepared with conditions M (41.94%) and L (40.86%).

Improved OsmY-DyP4 variants isolated from all epPCR conditions (H, M and L)

In total, we performed 3 rounds of random mutagenesis using epPCR. In the 1st and 2nd rounds, we screened 558 clones [2 96-well plates from each epPCR condition (H, M, L)]. In the 3rd round, 1116 clones [4 96-well plates from each epPCR condition (H, M, L)] were screened. The best variant from each epPCR round (OsmY-1D2 from 1st round and OsmY-2A5 from 2nd round) was used as parental template for the subsequent epPCR round. In the 4th round, we performed saturation mutagenesis on each mutated amino acid position identified (56, 109, 227, 306, 312 and 374), using OsmY-3F6 as template DNA.

As summarized in Table 2, OsmY-DyP4 variants with enhanced total activity under screening conditions were identified from all epPCR conditions (H, M, L). DNA sequencing of this set of improved variants showed that nucleotide substitutions were predominantly AT \rightarrow GC transitions (63.6%; Additional file 1: Table S1), consistent with the expected mutational spectrum of epPCR using Taq DNA polymerase (Wong et al. 2006; Tee and Wong 2013). On average, there were 1.82 nucleotide substitutions per DyP4 gene, which was deemed appropriate for directed evolution.

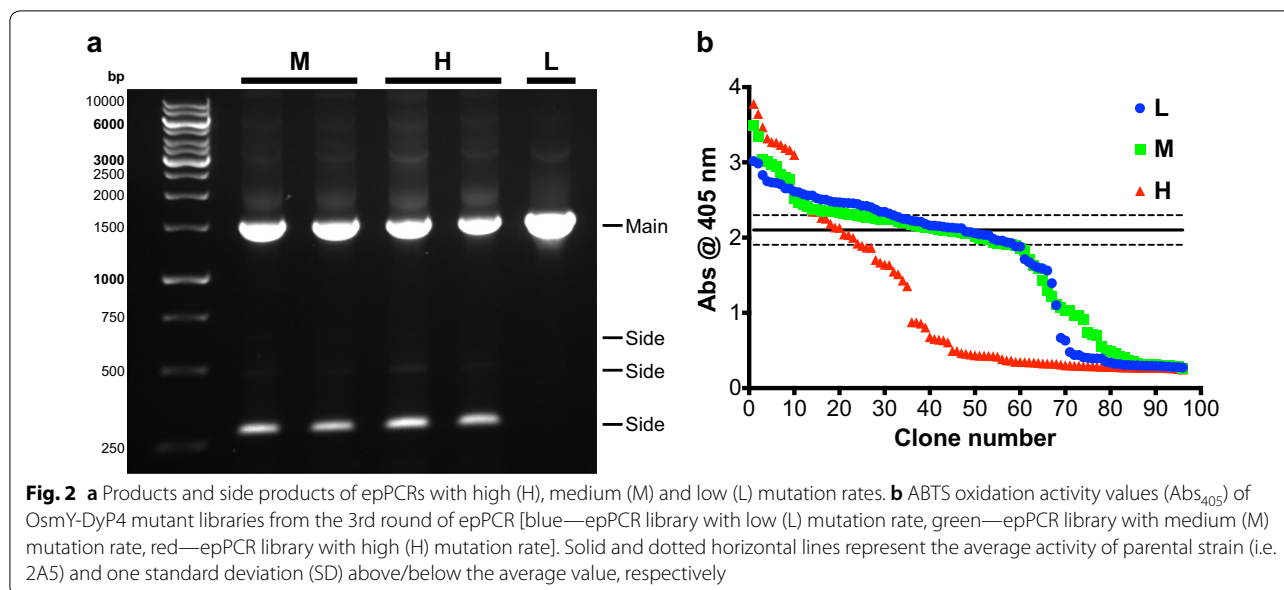


Table 2 A list of OsmY-DyP4 variants and the mutations in DyP4-coding sequences verified by DNA sequencing

OsmY-DyP4 and variants	Mutagenic rate of epPCR library	Missense mutations	Silent mutations
OsmY-WT*	N/A	N/A	N/A
OsmY-1D2*	L	<i>N312S (A→G)</i>	<i>D241 (T→C)</i> <i>I444 (C→T)</i>
OsmY-1D7	H	<i>A306V (C→T)</i>	<i>R323 (T→C)</i>
OsmY-2A5*	M	<i>I56V (A→G)</i> <i>N312S (A→G)</i>	<i>D241 (T→C)</i> <i>I444 (C→T)</i> <i>G73 (T→A)</i> <i>L245 (G→T)</i>
OsmY-2C2	M	<i>H374R (A→G)</i> <i>N312S (A→G)</i>	<i>D241 (T→C)</i> <i>I444 (C→T)</i>
OsmY-2F8	H	<i>N227D (A→G)</i> <i>N312S (A→G)</i>	<i>D241 (T→C)</i> <i>I444 (C→T)</i>
OsmY-3F6*	L	<i>K109R (A→G)</i> <i>N312S (A→G)</i> <i>I56V (A→G)</i>	<i>D241 (T→C)</i> <i>I444 (C→T)</i> <i>G73 (T→A)</i> <i>L245 (G→T)</i>
OsmY-4D4	N/A	<i>N227S</i> <i>N312S (A→G)</i> <i>I56V (A→G)</i> <i>K109R (A→G)</i>	<i>D241 (T→C)</i> <i>I444 (C→T)</i> <i>G73 (T→A)</i> <i>L245 (G→T)</i>

Clones labelled with an asterisk * were used as parental template for the subsequent round of mutagenesis; mutations in italics represent nucleotide substitutions added to a parental template

The best variant, OsmY-4D4, carries 4 amino acid substitutions (I56V, K109R, N227S and N312S; Fig. 3 and Additional file 1: Figure S6) along with 4 other silent mutations (Table 2). The crystal structures of F194Y (PDB 6FSK) and F194W (PDB 6FSL) variants of DyP4 were recently released. Residues 56 and 109 are located within α -helices, while the other two residues

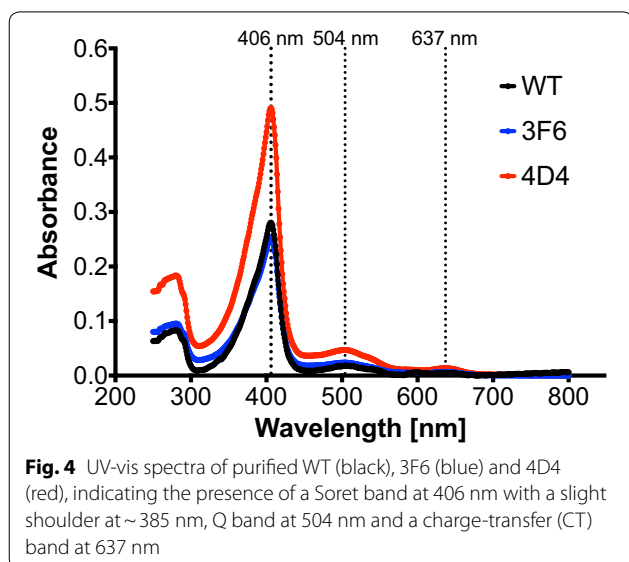
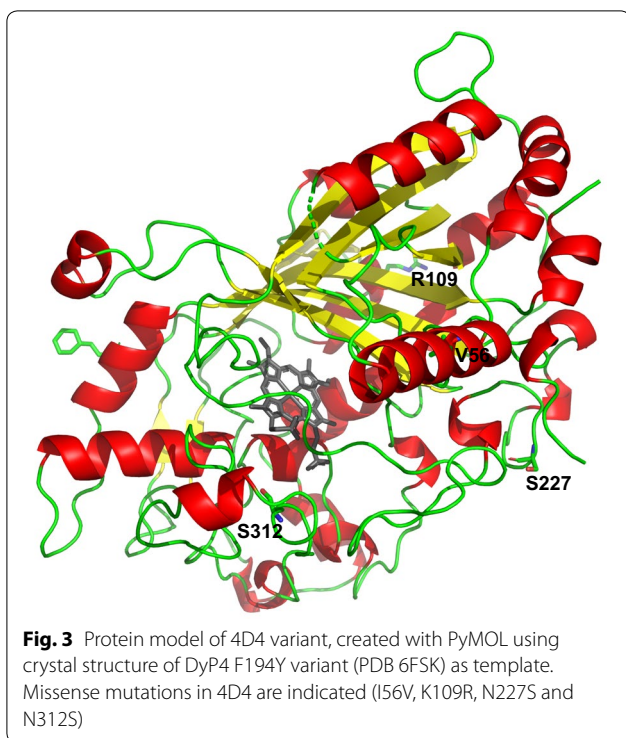
(227 and 312) are located in turns. None of these residues is in the vicinity of haem.

To further investigate the amino acid substitutions found in directed evolution, we looked at 3 aspects more closely solvent accessibility, B-factor and H-bond formation. Of the 4 residues, residue 109 is the only surface-exposed residue. The average B-factor of residue 109 (21.5678) is also slightly higher than protein average (21.146) and those of residues 56 (17.6775), 227 (15.9750) and 312 (15.4975). Interestingly, K109R and N312S substitutions resulted in higher number of H-bonds formed (3 H-bonds in R109 vs. 1 H-bond in K109 and 4 H-bonds in S312 vs. 3 H-bonds in N312).

DyP4 variants showed higher protein yield, specific activity and H₂O₂ tolerance

The enhanced total activity of OsmY-DyP4 variants in Table 2 could be due to one or more of the following factors: (1) increased protein expression or yield, (2) enhanced H₂O₂ tolerance and (3) increased extracellular protein secretion. To determine the effects of mutations found, we removed the N-terminal OsmY of WT, 3F6 and 4D4, expressed and purified these 3 proteins, and performed further characterizations.

Judging on the reddish colour of the cell pellets (Additional file 1: Figure S7) and the protein content of cell extract (Additional file 1: Figure S8), the protein yield of 3F6 and 4D4 was higher than that of WT. From 200-mL shake flask cultures, the estimated amounts of purified protein obtained were 1.16 mg for WT, 1.20 mg for 3F6 and 2.70 mg for 4D4. This could potentially explain marginally higher protein secretion that we observed for



OsmY-3F6 and OsmY-4D4 when we loaded the acetone-precipitated protein samples onto SDS-PAGE (Additional file 1: Figure S9). After protein purification, all 3 purified proteins exhibited a distinctive Soret band at 406 nm with a slight shoulder at ~385 nm (Fig. 4). Q band at 504 nm and a charge-transfer (CT) band at 637 nm were also clearly visible.

Using the purified proteins, we investigated the kinetic parameters for ABTS oxidation (Table 3). The k_{cat} values

of 3F6 and 4D4 were found to be 5.02 s^{-1} and 4.52 s^{-1} , respectively. These are slightly higher than WT's k_{cat} of 3.86 s^{-1} . Variants 3F6 and 4D4 showed lower K_m values of 0.427 mM and 0.390 mM, respectively, compared to WT (0.895 mM). This was unexpected as we used a relatively high ABTS concentration in our HTS, 6.8 mM, which is $7.6\times$ above the WT's K_m value. In fact, the WT's K_m value we determined (0.895 mM) was almost identical to a previously reported value (0.779 mM) (Fernandez-Fueyo et al. 2015). The combination of higher k_{cat} and lower K_m resulted in a 2.7-fold improvement in specific activity for both 3F6 and 4D4.

We also conducted ABTS assay in the presence of increasing H_2O_2 concentration (0.15–50.00 mM), with ABTS concentration kept at 7 mM. In Fig. 5, the activities at 0.25 mM H_2O_2 (the most optimal H_2O_2 concentration for ABTS oxidation) for WT and variants were arbitrarily set as 100% and used as reference points. Activities of WT, 3F6 and 4D4 at all other H_2O_2 concentrations were benchmarked against their respective reference. It became immediately apparent that the curves corresponding to 3F6 and 4D4 were shifted upwards and rightwards, indicating higher activity, a shift to higher optimal H_2O_2 concentration and higher H_2O_2 tolerance. Upon fitting the curves to an inhibitory dose–response curve with a variable slope (4 parameters), the IC_{50} value was increased from 0.97 mM (WT) to 4.67 mM (3F6) and 7.03 mM (4D4), as summarized in Table 4. In other words, the H_2O_2 tolerance of 4D4 was improved $7\times$, comparing its IC_{50} value to that of WT.

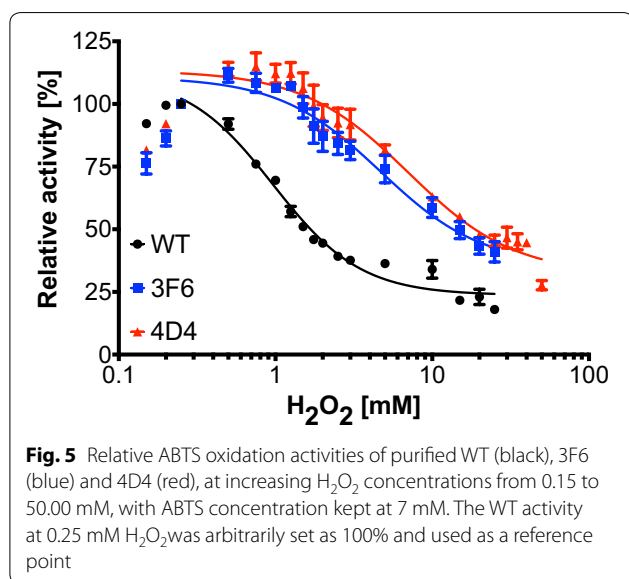
Protein production rate is likely faster than protein secretion rate

When we compared the cell pellets of DyP4 and variants with or without N-terminal OsmY fusion partner (Additional file 1: Figure S7), we noticed apparent colour difference between the two sets. The set with OsmY displayed much lighter reddish colour, which was expected for a system that allows extracellular protein secretion. Consistent with the set without OsmY, OsmY-3F6 and OsmY-4D4 showed slightly darker reddish colour compared to OsmY-WT, again suggesting higher protein yield of these two variants. This result also indicated that a portion of OsmY-DyP4 was not secreted. To understand the reason behind, we purified the OsmY-DyP4 from the cell pellets by following the identical protein purification scheme as DyP4.

In the final size exclusion chromatographic (SEC) step, we noticed that the haem-containing protein peak had a slight right shoulder (Additional file 1: Figure S10), indicating the presence of a slightly smaller protein. This was further confirmed when we loaded all collected protein fractions (F2 to F7) onto

Table 3 Kinetic parameters for ABTS oxidation of DyP4 and its variants

DyP4 and variants	K_m (mM)	V_{max} (mM ⁻¹ s ⁻¹)	k_{cat} (s ⁻¹)	k_{cat}/K_m (mM ⁻¹ s ⁻¹)
WT	0.895 ± 0.065	6.779 ± 0.142 × 10 ⁻⁴	3.86 ± 0.08	4.31 ± 0.41
3F6	0.427 ± 0.055	6.877 ± 0.202 × 10 ⁻⁴	5.02 ± 0.15	11.78 ± 1.86
4D4	0.390 ± 0.059	6.966 ± 0.233 × 10 ⁻⁴	4.52 ± 0.15	11.60 ± 2.14

**Table 4 H₂O₂ tolerance data of DyP4 and its variants were fitted to an inhibitory dose–response curve with a variable slope (4 parameters), using GraphPad software**

Best fit values	WT	3F6	4D4
Bottom	23.7 ± 1.6	35.4 ± 8.9	32.0 ± 6.8
Top	111.7 ± 5.9	110.8 ± 4.4	113.3 ± 3.8
HillSlope	1.6 ± 0.2	1.3 ± 0.4	1.3 ± 0.3
IC ₅₀	0.97 ± 0.10	4.67 ± 1.06	7.03 ± 1.33
R ²	0.9680	0.9131	0.9315

SDS-PAGE, where we saw two distinct protein bands (Additional file 1: Figure S10). We excised the protein band in F2 (larger M_w) and the protein band in F7 (smaller M_w), and conducted proteomic analysis. Mass spectrometry data acquired by LC–MS/MS led to both F2 and F7 matching to the recombinant OsmY-DyP4, with a lower sequence coverage for F7 (71%) relative to F2 (89%). Overlaying identified peptides to the amino acid sequence of OsmY-DyP4 fusion protein (Fig. 6) suggests a potential N-terminal truncation of the F2

protein to generate the F7 protein. The data suggested that the truncation likely occurred within the first 50 amino acids of OsmY. In other words, the signal peptide of OsmY (positions 1–28) was proteolytically cleaved, resulting in no secretion of this truncated protein pool. This signal peptide of OsmY was previously shown to play a key role in protein secretion (Qian et al. 2008).

Taken together, our experimental data suggested that (1) protein production rate of OsmY-DyP4 is likely faster than its extracellular secretion rate, and (2) the N-terminal region of OsmY, which encompasses its first 28 amino acids, is susceptible to proteolytic cleavage. These two factors potentially contribute to retention of small amount of DyP4 within the cell.

Conclusion

In conclusion, we were able to apply *E. coli* OsmY in a BENNY-assisted HTS system to significantly streamline the workflow of directed DyP4 evolution. Using this simplified scheme, we successfully isolated DyP4 variants that show multiple desirable phenotypes including higher protein yield, higher specific activity and higher H₂O₂ tolerance. We are now further engineering 4D4 variant for the oxidation of S-type phenolic lignin units (Camarero et al. 1994; Pardo et al. 2013) such as syringaldehyde, acetosyringone and sinapic acid etc. (on-going work).

The application of OsmY-based BENNY can further be extended to engineering other enzyme types, expressing toxic proteins and simplifying downstream processing in recombinant enzyme production. We are currently expanding the BENNY toolbox by (1) identifying new secretory proteins, (2) engineering OsmY and other related proteins for higher secretory phenotypes and (3) extending the application of OsmY to other bacterial hosts, encompassing both Gram-positive and Gram-negative bacteria (on-going work). Concurrently, we see exciting development in the field of BENNY reported by other research groups, such as identification of useful secretory carriers [e.g. YebF (Zhang et al. 2006) and Hly (Ruano-Gallego et al. 2019)] and engineering *E. coli*

a Protein sequence coverage of fraction F2: 89%

Matched peptides shown in red.

1	MTMTRLKISK	TLLAVMLTSA	VATGSAYAEN	NAQTTNESAG	QKVDSSMNKV
51	GNFMDDSAIT	AKVKAALVDH	DNIKSTDISV	KTDQKVVTLS	GFVESQAQAE
101	EAVKVAKGVE	GVTSVSDKLH	VRDAKEGSVK	GYAGDTATTS	EIKAKLLADD
151	IVPSRHVKVE	TTDGVVQLSG	TVDSQAQSDR	AESIAKAVDG	VKSVKNDLKT
201	KGSGSMTPPA	PPLDLNNIQG	DILGGLPKRT	ETYFFFDVTN	VDQFKANMAH
251	FIPHIKTSAG	IIKDREAIKE	HKRQKKPGLV	PMAAVNVSFS	HLGLQKLGIT
301	DDLSDNAFTT	GQRKDAEILG	DPGSKNGDAF	TPAWEAPFLK	DIHGVIHVAG
351	DCHGSVNKKL	DEIKHIFGVG	TSHASISEVT	HVRGDVRPGD	VHAHEHFGFL
401	DGISNPAVEQ	FDQNPLPGQD	PIRPGFILAK	ENGDSRAAAR	PDWAKDGSFL
451	TFRYLFQMVP	EFDDFLESNP	IVLPGLSRKE	GSELLGARIV	GRWKS GAPIE
501	ITPLKDDPKL	AADAQRNKNF	DFGDSLVRGD	QTKCPFAAHI	RKTYPRNDLE
551	GPPLKADIDN	RRIIRRGIQF	GPEVTSQEHH	DKKTHHGRGL	LFVYSSSID
601	DGFHFIQESW	ANAPNFPVNA	VTSAGPIPPL	DGVVPGFDAI	IGQKVGGGIR
651	QISGTNPNDP	TTNITLDPQD	FVVPRGGEYF	FSPSITALKT	KFAIGVASPA
701	PHSQAPISA				

b Protein sequence coverage of fraction F7: 71%

Matched peptides shown in red.

1	MTMTRLKISK	TLLAVMLTSA	VATGSAYAEN	NAQTTNESAG	QKVDSSMNKV
51	GNFMDDSAIT	AKVKAALVDH	DNIKSTDISV	KTDQKVVTLS	GFVESQAQAE
101	EAVKVAKGVE	GVTSVSDKLH	VRDAKEGSVK	GYAGDTATTS	EIKAKLLADD
151	IVPSRHVKVE	TTDGVVQLSG	TVDSQAQSDR	AESIAKAVDG	VKSVKNDLKT
201	KGSGSMTPPA	PPLDLNNIQG	DILGGLPKRT	ETYFFFDVTN	VDQFKANMAH
251	FIPHIKTSAG	IIKDREAIKE	HKRQKKPGLV	PMAAVNVSFS	HLGLQKLGIT
301	DDLSDNAFTT	GQRKDAEILG	DPGSKNGDAF	TPAWEAPFLK	DIHGVIHVAG
351	DCHGSVNKKL	DEIKHIFGVG	TSHASISEVT	HVRGDVRPGD	VHAHEHFGFL
401	DGISNPAVEQ	FDQNPLPGQD	PIRPGFILAK	ENGDSRAAAR	PDWAKDGSFL
451	TFRYLFQMVP	EFDDFLESNP	IVLPGLSRKE	GSELLGARIV	GRWKS GAPIE
501	ITPLKDDPKL	AADAQRNKNF	DFGDSLVRGD	QTKCPFAAHI	RKTYPRNDLE
551	GPPLKADIDN	RRIIRRGIQF	GPEVTSQEHH	DKKTHHGRGL	LFVYSSSID
601	DGFHFIQESW	ANAPNFPVNA	VTSAGPIPPL	DGVVPGFDAI	IGQKVGGGIR
651	QISGTNPNDP	TTNITLDPQD	FVVPRGGEYF	FSPSITALKT	KFAIGVASPA
701	PHSQAPISA				

Fig. 6 Mass spectrometry data of SEC fractions F2 (a) and F7 (b) proteins. Mascot database searching against the *Escherichia coli* (strain B/BL21-DE3) reference proteome, plus the recombinant OsmY-DyP4 sequence, led to matching to this recombinant protein. Matched peptides are shown in red against the full-length amino acid sequence of the recombinant protein

cells showing hyper secretory phenotypes (e.g. *E. coli* BW25113 $\Delta yaiW$ and *E. coli* BW25113 $\Delta gfcC$) (Natarajan et al. 2017).

Additional file

Additional file 1. Supplementary material.

Abbreviations

Ab₅₄₀₅: absorbance at 405 nm; ABTS: 2,2'-azino-bis(3-ethylbenzothiazoline-6-sulphonic acid); AIM: auto induction medium; AnaPX: dye-decolorizing peroxidase from cyanobacterium *Anabaena* sp. strain PCC 7120; BENNY: bacterial extracellular protein secretion system; CV: coefficient of variance; CVs: column volumes; dATP: deoxyadenosine triphosphate; dCTP: deoxycytidine triphosphate; dGTP: deoxyguanosine triphosphate; DMP: 2,6-dimethoxyphenol; dNTP: deoxynucleotide; dTTP: deoxythymidine triphosphate; DyP: dye-decolorizing peroxidase; DyP4: dye-decolorizing peroxidase 4 from *Pleurotus* strain PC15; *E. coli*: *Escherichia coli*; epCPR: error-prone polymerase chain reaction; HTS: high-throughput screening; IC₅₀: half maximal inhibitory concentration; IPTG: isopropyl β-D-1-thiogalactopyranoside; LiP: lignin peroxidase; MnP: manganese peroxidase; M_w: molecular weight; OD₆₀₀: optical density at 600 nm; OsmY: osmotically-inducible protein Y; PCR: polymerase chain reaction; *P. ostreatus*: *Pleurotus ostreatus*; PpDyP: dye-decolorizing peroxidase from *Pseudomonas putida* MET94; RB5: Reactive Black 5; RB19: Reactive Blue 19; SDS-PAGE: sodium dodecyl sulphate polyacrylamide gel electrophoresis; SEC: size exclusion chromatography; WT: wildtype.

Acknowledgements

Not applicable.

Authors' contributions

TSW and KLT supervised the project and designed the experiments. AHAA, KLT, DGP, HEMOA, CE and AT conducted the experiments. TSW, KLT, CE and JX analysed the data and wrote the manuscript. All authors read and approved the final manuscript.

Funding

We thank the Department of Chemical and Biological Engineering, ChELSI, EPSRC (EP/E036252/1), the Open Project Funding of the State Key Laboratory of Bioreactor Engineering, The Leverhulme Trust Senior Research Fellowship (to TSW), University of Sheffield GCRF Fellowship (to KLT), BBSRC (BB/R020183/1), University of Tabuk, Singapore A*STAR and COST action (CM1303; Systems Biocatalysis) for financial support.

Availability of data and materials

Not applicable.

Ethics approval and consent to participate

Not applicable.

Consent for publication

All authors have read the manuscript and approved its submission to *Bioresour. Bioprocess.*

Competing interests

The authors declare that they have no competing interests.

Author details

¹ Department of Chemical & Biological Engineering and Advanced Biomanufacturing Centre, University of Sheffield, Sir Robert Hadfield Building, Mappin Street, Sheffield S1 3JD, UK. ² Laboratory of Biocatalysis and Bioprocessing, State Key Laboratory of Bioreactor Engineering, East China University of Science and Technology, 130 Meilong Road, Shanghai 200237, People's Republic of China.

Received: 15 April 2019 Accepted: 20 May 2019

Published online: 31 May 2019

References

- Brissos V, Tavares D, Sousa AC, Robalo MP, Martins LO (2017) Engineering a bacterial DyP-type peroxidase for enhanced oxidation of lignin-related phenolics at alkaline pH. *ACS Catal* 7:3454–3465
- Camarero S, Galletti GC, Martinez AT (1994) Preferential degradation of phenolic lignin units by two white rot fungi. *Appl Environ Microbiol* 60:4509–4516
- Cheng CM, Tzou SC, Zhuang YH, Huang CC, Kao CH, Liao KW, Cheng TC, Chuang CH, Hsieh YC, Tai MH, Cheng TL (2014) Functional production of a soluble and secreted single-chain antibody by a bacterial secretion system. *PLoS ONE* 9:e97367
- Fawal N, Li Q, Savelli B, Brette M, Passaia G, Fabre M, Mathe C, Dunand C (2013) PeroxiBase: a database for large-scale evolutionary analysis of peroxidases. *Nucleic Acids Res* 41:D441–444
- Fernandez-Fueyo E, Linde D, Almendral D, Lopez-Lucendo MF, Ruiz-Duenas FJ, Martinez AT (2015) Description of the first fungal dye-decolorizing peroxidase oxidizing manganese (II). *Appl Microbiol Biotechnol* 99:8927–8942
- Gupta S, Adlakha N, Yazdani SS (2013) Efficient extracellular secretion of an endoglucanase and a beta-glucosidase in *E. coli*. *Protein Expr Purif* 88:20–25
- Hofrichter M, Ullrich R, Pecyna MJ, Liers C, Lundell T (2010) New and classic families of secreted fungal heme peroxidases. *Appl Microbiol Biotechnol* 87:871–897
- Kotzsch A, Vernet E, Hammarstrom M, Berthelsen J, Weigelt J, Graslund S, Sundstrom M (2011) A secretory system for bacterial production of high-profile protein targets. *Protein Sci* 20:597–609
- Le Y, Wang H (2014) High-level soluble expression of a thermostable xylanase from thermophilic fungus *Thermomyces lanuginosus* in *Escherichia coli* via fusion with OsmY protein. *Protein Expr Purif* 99:1–5
- Li S, Schoneich C, Borchardt RT (1995) Chemical instability of protein pharmaceuticals: mechanisms of oxidation and strategies for stabilization. *Biotechnol Bioeng* 48:490–500
- Martinez AT, Ruiz-Duenas FJ, Camarero S, Serrano A, Linde D, Lund H, Vind J, Tovborg M, Herold-Majumdar OM, Hofrichter M, Liers C, Ullrich R, Scheibner K, Sannia G, Piscitelli A, Pezzella C, Sener ME, Kilic S, van Berkel WJH, Guallar V, Lucas MF, Zuhse R, Ludwig R, Hollmann F, Fernandez-Fueyo E, Record E, Faulds CB, Tortajada M, Winkelmann I, Rasmussen JA, Gelo-Pujic M, Gutierrez A, Del Rio JC, Rencoret J, Alcalde M (2017) Oxidoreductases on their way to industrial biotransformations. *Biotechnol Adv* 35:815–831
- Natarajan A, Haitjema CH, Lee R, Boock JT, DeLisa MP (2017) An engineered survival-selection assay for extracellular protein expression uncovers hypersecretory phenotypes in *Escherichia coli*. *ACS Synth Biol* 6:875–883
- Ogola HJ, Kamiike T, Hashimoto N, Ashida H, Ishikawa T, Shibata H, Sawa Y (2009) Molecular characterization of a novel peroxidase from the cyanobacterium *Anabaena* sp. strain PCC 7120. *Appl Environ Microbiol* 75:7509–7518
- Ogola HJ, Hashimoto N, Miyabe S, Ashida H, Ishikawa T, Shibata H, Sawa Y (2010) Enhancement of hydrogen peroxide stability of a novel *Anabaena* sp. DyP-type peroxidase by site-directed mutagenesis of methionine residues. *Appl Microbiol Biotechnol* 87:1727–1736
- Otieno BA, Krause CE, Rusling JF (2016) Bioconjugation of antibodies and enzyme labels onto magnetic beads. *Methods Enzymol* 571:135–150
- Pardo I, Chanaga X, Vicente AI, Alcalde M, Camarero S (2013) New colorimetric screening assays for the directed evolution of fungal laccases to improve the conversion of plant biomass. *BMC Biotechnol* 13:90
- Qian ZG, Xia XX, Choi JH, Lee SY (2008) Proteome-based identification of fusion partner for high-level extracellular production of recombinant proteins in *Escherichia coli*. *Biotechnol Bioeng* 101:587–601
- Ruano-Gallego D, Fraile S, Gutierrez C, Fernandez LA (2019) Screening and purification of nanobodies from *E. coli* culture supernatants using the hemolysin secretion system. *Microb Cell Fact* 18:47

- Salvachua D, Prieto A, Martinez AT, Martinez MJ (2013) Characterization of a novel dye-decolorizing peroxidase (DyP)-type enzyme from *Irpelex lacteus* and its application in enzymatic hydrolysis of wheat straw. *Appl Environ Microbiol* 79:4316–4324
- Shevchenko A, Tomas H, Havlis J, Olsen JV, Mann M (2006) In-gel digestion for mass spectrometric characterization of proteins and proteomes. *Nat Protoc* 1:2856–2860
- Singh R, Eltis LD (2015) The multihued palette of dye-decolorizing peroxidases. *Arch Biochem Biophys* 574:56–65
- Tee KL, Wong TS (2013) Polishing the craft of genetic diversity creation in directed evolution. *Biotechnol Adv* 31:1707–1721
- Warburton M, Omar Ali H, Liong WC, Othuisitse AM, Abdullah Zubir AZ, Maddock S, Wong TS (2015) OneClick: a program for designing focused mutagenesis experiments. *AIMS Bioengineering* 2:126–143
- Wong TS, Zhurina D, Schwaneberg U (2006) The diversity challenge in directed protein evolution. *Comb Chem High Throughput Screen* 9:271–288
- Zhang G, Brokx S, Weiner JH (2006) Extracellular accumulation of recombinant proteins fused to the carrier protein YebF in *Escherichia coli*. *Nat Biotechnol* 24:100–104
- Zheng Z, Chen T, Zhao M, Wang Z, Zhao X (2012) Engineering *Escherichia coli* for succinate production from hemicellulose via consolidated bio-processing. *Microb Cell Fact* 11:37

Publisher's Note

Springer Nature remains neutral with regard to jurisdictional claims in published maps and institutional affiliations.

Submit your manuscript to a SpringerOpen[®] journal and benefit from:

- Convenient online submission
- Rigorous peer review
- Open access: articles freely available online
- High visibility within the field
- Retaining the copyright to your article

Submit your next manuscript at ► [springeropen.com](https://www.springeropen.com)
